

## Synthesis of Nano-sized Tabular Lindgrenite ( $\text{Cu}_3(\text{MoO}_4)_2(\text{OH})_2$ ) by Aqueous Precipitation

JIANG Wen-Jun<sup>1,2,3</sup>, FANG Jin<sup>2</sup>, FAN Zhong-Yong<sup>1</sup>, YANG Xu-Jie<sup>2</sup>, LU Qi-Ting<sup>3</sup>, HOU Yi-Bin<sup>3</sup>

(1. Department of Materials Science, Fudan University, Shanghai 200433, China; 2. Key Laboratory for Soft Chemistry and Functional Materials, Ministry of Education, Nanjing University of Science and Technology, Nanjing 210094, China; 3. Shanghai Kangda Chemical Co., LTD, Shanghai 201201, China)

**Abstract:** Lindgrenite ( $\text{Cu}_3(\text{MoO}_4)_2(\text{OH})_2$ ) nanocrystals were synthesized by simple aqueous precipitation at 60 °C, using  $\text{Cu}(\text{NO}_3)_2 \cdot 6\text{H}_2\text{O}$ ,  $\text{Na}_2\text{MoO}_4 \cdot 2\text{H}_2\text{O}$  and NaOH as the starting materials. X-ray Diffraction (XRD) patterns confirm the formation of pure  $\text{Cu}_3(\text{MoO}_4)_2(\text{OH})_2$  nanocrystals, which belongs to the monoclinic phase with calculated crystal parameters  $a = 0.53863 \text{ nm}$ ,  $b = 1.40006 \text{ nm}$ ,  $c = 0.56003 \text{ nm}$ ,  $\beta = 98.47^\circ$ ,  $\alpha = \gamma = 90^\circ$ . The energy dispersive X-ray spectrum (EDX) analysis gives an approximate atomic ratio of 3:2:10 for Cu: Mo: O. The scanning electron microscope (SEM) and transmission electron microscope (TEM) studies show that the as-prepared nanoparticles are well crystallized with tabular structure and the interplanar distances of  $d_{021}$  and  $d_{121}$  measured are 0.435 nm and 0.358 nm, coinciding with the theoretical value. It can also be seen that the  $\text{Cu}_3(\text{MoO}_4)_2(\text{OH})_2$  has a good thermal stability and starts decomposing at 320 °C through thermogravimetric-differential thermal analysis (TG-DTA). Moreover, the strong fluorescent property of the  $\text{Cu}_3(\text{MoO}_4)_2(\text{OH})_2$  is measured, with green emission peak at ca. 530 nm upon excitation at ca. 369 nm. Finally, a possible mechanism for the formation of  $\text{Cu}_3(\text{MoO}_4)_2(\text{OH})_2$  nanocrystals is proposed.

**Key words:** lindgrenite ( $\text{Cu}_3(\text{MoO}_4)_2(\text{OH})_2$ ); aqueous precipitation; nanocrystals; characterization; thermal stability; fluorescent property

Detailed knowledge on the stability and formation conditions of mineral is of great importance, both for the understanding of geological processes<sup>[1]</sup> as well as to optimize performance of minerals in industrial applications<sup>[2]</sup>. Lindgrenite ( $\text{Cu}_3(\text{MoO}_4)_2(\text{OH})_2$ ) has been shown to be an effective fire retardant and smoke suppressor when combined with  $\text{CuSnO}_3$  in polyvinyl chloride plastic (PVC)<sup>[3]</sup>.

Lindgrenite ( $\text{Cu}_3(\text{MoO}_4)_2(\text{OH})_2$ ) is one kind of rare mineral originally found in Chile resulting from the oxidation of primary molybdenite<sup>[4]</sup>. Early in 1980, Moini *et al*<sup>[5]</sup> synthesized  $\text{Cu}_3(\text{MoO}_4)_2(\text{OH})_2$  using  $\text{CuSO}_4$  and  $\text{Na}_2\text{MoO}_4$  as raw materials under aqueous reflux conditions, and the obtained products were studied by XRD and TGA. Recently, many researchers<sup>[6-8]</sup> are shifting their interests toward hydrothermal method in preparing  $\text{Cu}_3(\text{MoO}_4)_2(\text{OH})_2$ . There are still no more detailed reports about the synthesis and the morphology of  $\text{Cu}_3(\text{MoO}_4)_2(\text{OH})_2$  nanomaterials with precipitation method at low temperature<sup>[9]</sup>.

As reinforcing agents or flame-retardants, it seems that

the needle-like and the sheet-like structure materials are good candidates for functional polymeric composites and fiber hybrid materials<sup>[10-11]</sup>. In our work, the tabular  $\text{Cu}_3(\text{MoO}_4)_2(\text{OH})_2$  nanocrystals were synthesized with relatively large quantity by aqueous precipitation at 60 °C. This method is cost-effective and available to a large-scale production. The as-prepared products were characterized by SEM, TEM, HTEM, EDX, XRD, FTIR, TG-DTA and Emission/excitation spectra.

## 1 Experimental

### 1.1 Materials and Preparation

All chemicals were of analytical grade and were used without further purification.  $\text{Cu}_3(\text{MoO}_4)_2(\text{OH})_2$  nanocrystals were prepared by aqueous precipitation. 0.04 mol  $\text{Na}_2\text{MoO}_4 \cdot 2\text{H}_2\text{O}$  and 0.04 mol NaOH were dissolved in the 50 mL deionized water, and then 50 mL  $\text{Cu}(\text{NO}_3)_2$  solution (1.2 mol/L) was added dropwise under mechanical agitation at 25 °C. Next,  $\text{HNO}_3$  and NaOH were separately

Received date: 2010-11-04; Modified date: 2010-12-13; Published online: 2010-12-30

Foundation item: High Technical Foundation of Jiangsu Province (BG2007047); National Natural Science Foundation of China (50772048)

Biography: JIANG Wen-Jun (1980-), male, PhD. E-mail: jwj80927@tom.com

Corresponding author: FANG Zhong-Yong, professor. E-mail: zyfan@fudan.edu.cn; Xujie Yang, professor. E-mail: yangx@mail.njust.edu.cn

added to keep pH=6. Afterwards, the whole solution was divided into three parts and aged for 3 h at 25 °C, 45 °C and 60 °C, respectively. Finally, the obtained products were washed with deionized water for three times and dried at 25 °C in vacuum.

## 1.2 Characterization methods

The X-ray diffraction patterns (XRD) were carried out on a Bruker D8 Advanced X-ray diffractometer using  $\text{Cu K}\alpha$  radiation ( $\lambda=0.15406$  nm) with the range of the diffraction angle of  $2\theta = 10^\circ\text{--}60^\circ$ . Fourier transform infrared (FTIR) spectrum of KBr powder-pressed pellets was recorded on a Bruker Vector 22 spectrometer. SEM image and Energy dispersive X-ray spectrum (EDX) analysis<sup>[12]</sup> were obtained on a LEO-1550VP scanning electron microscope. TEM and HRTEM were taken with a JEOL JEM-2100 electron microscope. Thermogravimetric-differential thermal analysis (TG-DTA) was performed on a Beijing WCT-2A thermal analyzer at 60–950 °C at a heating rate of 20 °C/min in air. Emission/excitation spectra were recorded on a FL3-TCSPC fluorescence spectrophotometer at room temperature.

## 2 Results and discussion

SEM image (Fig. 1(a)) of the  $\text{Cu}_3(\text{MoO}_4)_2(\text{OH})_2$  prepared at 60 °C demonstrates that the nanocrystals are tabular with the sizes of 50–100 nm in width and 100–300 nm in length, and that also can be confirmed by the TEM results in Fig. 1(b). The HRTEM image (Fig. 1(c)) clearly reveals that the as-prepared product is well crystalline, and the lattice fringes with the interplanar distance of 0.435 nm and 0.358 nm are assigned to the (021) plane and  $(\bar{1}21)$  plane of monoclinic  $\text{Cu}_3(\text{MoO}_4)_2(\text{OH})_2$  structure, implying that high quality monoclinic  $\text{Cu}_3(\text{MoO}_4)_2(\text{OH})_2$  nanocrystals are formed.

EDX analysis is performed to further confirm the composition of the obtained product<sup>[12]</sup>. Figure 2 indicate that the product is composed of Cu, Mo, and O, with an approximate molar ratio of 3:2:10, according with corresponding molecular formula  $\text{Cu}_3(\text{MoO}_4)_2(\text{OH})_2$ . The C peak in the spectrum is attributed to the electric latex of the SEM sample holder and the Pt peaks come from the Pt sputtering process in SEM experiment.

The XRD patterns (Fig. 3(a)) confirm the presence of pure lindgrenite,  $\text{Cu}_3(\text{MoO}_4)_2(\text{OH})_2$  (JCPDS file 75-1438). It can be clearly seen that with increasing the aging temperature from 25 °C to 60 °C, the products become better crystallized with the obvious enhancement in several peaks such as 12.62°, 20.42° and 24.85°, which are also

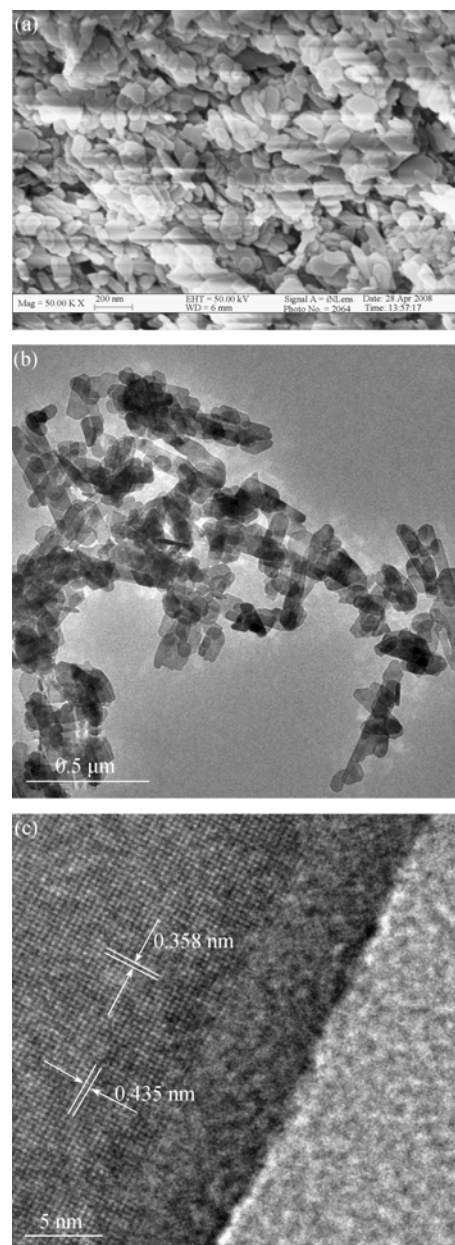


Fig. 1 (a) SEM, (b) TEM and (c) HTEM images of synthetic lindgrenite precipitated from aqueous solution at 60 °C

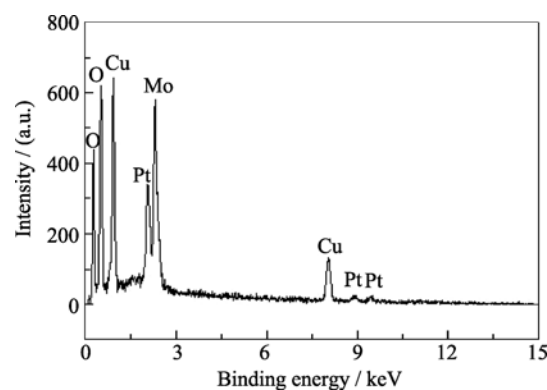


Fig. 2 EDX spectrum of synthetic lindgrenite precipitated from aqueous solution at 60 °C

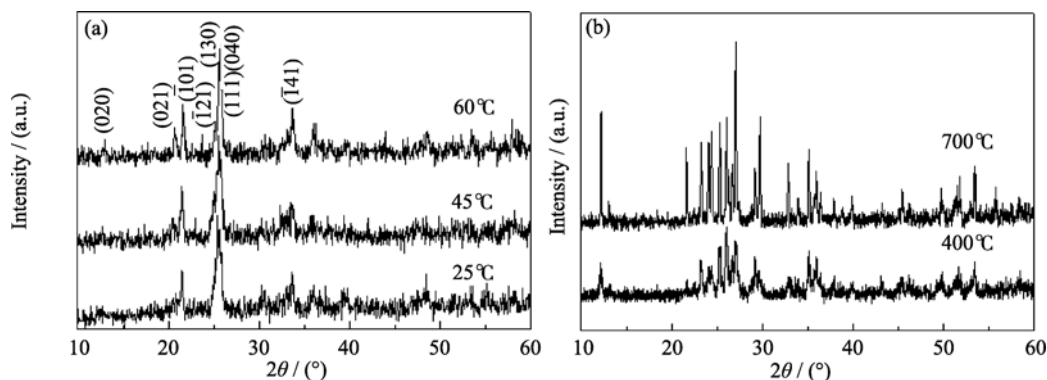


Fig. 3 XRD patterns of (a) lindgrenite nanocrystals and (b)  $\text{Cu}_3\text{Mo}_2\text{O}_9$  powders

confirmed by the HRTEM image. The calculated crystal parameters of the as-prepared lindgrenite by Fullprof program are shown that  $a = 0.53863$  nm,  $b = 1.40006$  nm,  $c = 0.56003$  nm,  $\beta = 98.47^\circ$ ,  $\alpha = \gamma = 90^\circ$ , which also suggests that the product belongs to the monoclinic crystal system. The eight main peaks at  $2\theta$  values of  $12.62^\circ$ ,  $20.42^\circ$ ,  $21.34^\circ$ ,  $24.85^\circ$ ,  $25.34^\circ$ ,  $25.42^\circ$ ,  $25.62^\circ$  and  $33.43^\circ$  are indexed as (020), (021), (101), (121), (130), (040), (111) and (141) of  $\text{Cu}_3(\text{MoO}_4)_2(\text{OH})_2$ , respectively, which are in agreement with the data of the reported literature<sup>[13]</sup>. The results indicate that pure  $\text{Cu}_3(\text{MoO}_4)_2(\text{OH})_2$  is synthesized by aqueous precipitation at a relatively lower preparing temperature ( $60^\circ\text{C}$ ). In addition, Fig. 3(b) shows the generation of  $\text{Cu}_3\text{Mo}_2\text{O}_9$  after the product is calcined at  $400^\circ\text{C}$  and  $700^\circ\text{C}$  in air for 20 min, corresponding to the orthorhombic structure<sup>[7]</sup> with lattice constants of  $a = 0.7659$  nm,  $b = 1.4613$  nm, and  $c = 0.6875$  nm (JCPDS file 70-2493). Those are in good agreement with the theoretical decomposition product of  $\text{Cu}_3(\text{MoO}_4)_2(\text{OH})_2$ .

The FTIR spectrum of  $\text{Cu}_3(\text{MoO}_4)_2(\text{OH})_2$  nanocrystals is detected in Fig. 4. The bands at 386, 825, 869, 916 and  $968\text{ cm}^{-1}$  are ascribed to  $\text{MoO}_4^{2-}$  vibration, consistent with the reported values<sup>[6]</sup>. The bands at 420 and  $3346\text{ cm}^{-1}$  can be assigned to O–H vibration. The absorption peak at  $459\text{ cm}^{-1}$  is from the bending vibration of Cu–O. In addition, the weak absorption at  $1633\text{ cm}^{-1}$  and the peaks at  $3000 - 3600\text{ cm}^{-1}$  may be caused by the bending vibration and the stretching vibration of  $\text{H}_2\text{O}$ , respectively<sup>[14-15]</sup>.

TG-DTA curves obtained under a flow of air are shown in Fig. 5. The TG curve records a weight loss between  $320^\circ\text{C}$  and  $400^\circ\text{C}$ , corresponding to the departure of OH groups as  $\text{H}_2\text{O}$  by 3.33wt% weight loss, which shows that  $\text{Cu}_3(\text{MoO}_4)_2(\text{OH})_2$  is decomposed into  $\text{Cu}_3\text{Mo}_2\text{O}_9$  and  $\text{H}_2\text{O}$  in line with the XRD results. A second weight loss by 3.39wt% takes place between  $850^\circ\text{C}$  and  $900^\circ\text{C}$ , which may be related to the decomposition of  $\text{Cu}_3\text{Mo}_2\text{O}_9$ <sup>[6]</sup>. The DTA curve exhibits two distinct endothermic peaks centered at  $378^\circ\text{C}$  and  $890^\circ\text{C}$ , which are assigned to the de-

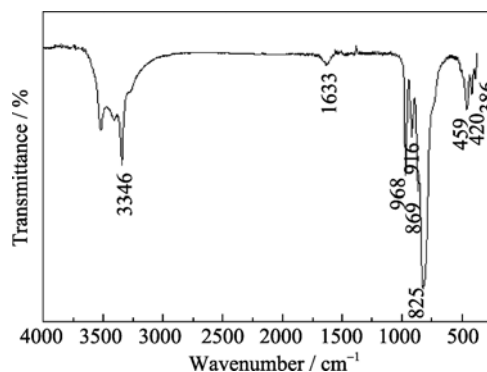


Fig. 4 Transmittance FT-IR spectrum of synthetic lindgrenite precipitated from aqueous solution at  $60^\circ\text{C}$

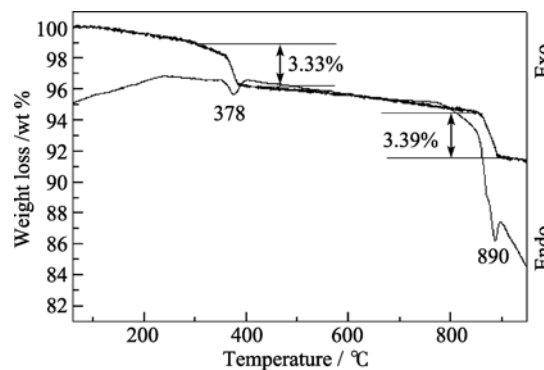


Fig. 5 Weight loss by TG-DTA of synthetic lindgrenite precipitated from aqueous solution at  $60^\circ\text{C}$

hydration of lindgrenite and phase transition of the remainder, respectively.

The fluorescent property of the  $\text{Cu}_3(\text{MoO}_4)_2(\text{OH})_2$  nanocrystals prepared at  $60^\circ\text{C}$  is measured at room temperature. As shown in Fig. 6, with the excited wavelength at *ca.*  $369\text{ nm}$ , the nanocrystals exhibit green emission peak at *ca.*  $530\text{ nm}$ , which could be due to the charge-transfer transitions within the  $\text{MoO}_4^{2-}$  complex<sup>[16-17]</sup>. The results also indicate that  $\text{Cu}_3(\text{MoO}_4)_2(\text{OH})_2$  nanocrystals prepared by this method are a kind of potential fluorescent-emitted material.

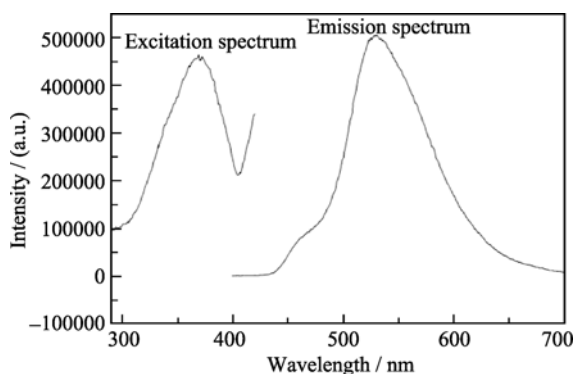
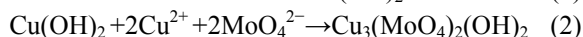


Fig. 6 Solid-state emission/excitation spectrum of synthetic lindgrenite precipitated from aqueous solution at 60 °C

The formation process of  $\text{Cu}_3(\text{MoO}_4)_2(\text{OH})_2$  nanocrystals could be described as follows: when  $\text{Cu}(\text{NO}_3)_2$  solution was added to the  $\text{MoO}_4^{2-}$  solution, it was possible that  $\text{Cu}(\text{OH})_2$  formed firstly, and then  $\text{Cu}(\text{OH})_2$  combined with copper ions and  $\text{MoO}_4^{2-}$  to generate  $\text{Cu}_3(\text{MoO}_4)_2(\text{OH})_2$  nanocrystals from color change of the suspension (blue  $\rightarrow$  yellow-green), as described in Equations (1) and (2).



The proposed reaction mechanism has been supported by the following experiment that  $\text{Cu}_3(\text{MoO}_4)_2(\text{OH})_2$  nanocrystals also can be synthesized by adding  $\text{Na}_2\text{MoO}_4$  into the  $\text{Cu}(\text{OH})_2$  suspending solution prepared by prior adding  $\text{Cu}^{2+}$  into NaOH solution.

### 3 Conclusion

In this study, the tabular and well-crystalline monoclinic  $\text{Cu}_3(\text{MoO}_4)_2(\text{OH})_2$  nanocrystals have been prepared via a simple route based on precipitation method at 60 °C, employing  $\text{Cu}(\text{NO}_3)_2 \cdot 6\text{H}_2\text{O}$ ,  $\text{Na}_2\text{MoO}_4 \cdot 2\text{H}_2\text{O}$  and NaOH as the starting materials. This method is highly promising to be scaled up for industrial application owing to the short reaction time and the simple synthetic process.

### References:

- [1] Winkler H G F. *Petrogenesis of Metamorphic rock*, 5th ed. New York: Springer Verlag, 1979: 472.
- [2] Chang L L Y. *Industrial Mineralogy. Materials, Processes, and*

- Uses*. Prentice Hall, Upper Saddle River, New Jersey, 2002: 472.
- [3] Starnes Jr W H, Pike R D, Cole J R, *et al.* Cone calorimetric study of copper-promoted smoke suppression and fire retardance of poly(vinyl chloride). *Polym. Degrad. Stab.*, 2003, **82(1)**: 15–24.
- [4] Palache C. Lindgrenite, a new mineral. *Am. Mineral.*, 1935, **20(7)**: 484–491.
- [5] Moini A, Peascoe R, Rudolf P R, *et al.* Hydrothermal synthesis of copper molybdates. *Inorg. Chem.*, 1986, **25(21)**: 3782–3785.
- [6] Vilminot S, André G, Richard-Plouet M, *et al.* Magnetic structure and magnetic properties of synthetic lindgrenite,  $\text{Cu}_3(\text{OH})_2(\text{MoO}_4)_2$ . *Inorg. Chem.*, 2006, **45(26)**: 10938–10946.
- [7] Bao R L, Kong Z P, Gu M, *et al.* Hydrothermal synthesis and thermal stability of natural mineral lindgrenite. *Chem. Res. Chinese U.*, 2006, **22(6)**: 679–683.
- [8] Shores M P, Bartlett B M, Nocera D G. Spin-frustrated organic-inorganic hybrids of lindgrenite. *J. Am. Chem. Soc.*, 2005, **127(51)**: 17986–17987.
- [9] Xu J S, Xue D F. Hydrothermal synthesis of lindgrenite with a hollow and prickly sphere-like architecture. *J. Solid State Chem.*, 2007, **180(1)**: 119–126.
- [10] Alexandre M, Beyer G, Henrist C, *et al.* Preparation and properties of layered silicate nanocomposites based on ethylene vinyl acetate copolymers. *Macromol. Rapid Commun.*, 2001, **22(8)**: 643–646.
- [11] Li H Y, Chen Y F, Xie Y S. Photo-crosslinking polymerization to prepare polyanhydride/needle-like hydroxyapatite biodegradable nanocomposite for orthopedic application. *Mater. Lett.*, 2003, **57(19)**: 2848–2854.
- [12] Frost R L, Duong L, Weier M. Raman microscopy of the molybdate minerals koechlinite, iriginite and lindgrenite. *Neues Jahrbuch fuer Mineralogie, Abhandlungen*, 2004, **180(3)**: 245–260.
- [13] Calvert L D, Barnes W H. The structure of Lindgrenite. *Can. Mineral.*, 1957, **6**: 31–51.
- [14] Jiang W J, Hua X, Han Q F, *et al.* Preparation of lamellar magnesium hydroxide nanoparticles via precipitation method. *Powder Technol.*, 2009, **191(3)**: 227–230.
- [15] Hassanzadeh-Tabrizi S A, Taheri-Nassaj E, Sarpoolaky H. Synthesis of an alumina-YAG nanopowder via Sol-Gel method. *J. Alloys Compd.*, 2008, **456(1/2)**: 282–285.
- [16] Ryu J H, Yoon J W, Lim C S, *et al.* Microwave-assisted synthesis of barium molybdate by a citrate complex method and oriented aggregation. *Mater. Res. Bull.*, 2005, **40(1)**: 1468–1476.
- [17] Sczancoski JC, Cavalcante L S, Joya M R, *et al.*  $\text{SrMoO}_4$  powders processed in microwave-hydrothermal: synthesis, characterization and optical properties. *Chem. Eng. J.*, 2008, **140(1/2/3)**: 632–637.

# 水相沉淀法制备纳米片状钼铜矿( $\text{Cu}_3(\text{MoO}_4)_2(\text{OH})_2$ )

蒋文俊<sup>1,2,3</sup>, 方 劲<sup>2</sup>, 范仲勇<sup>1</sup>, 杨绪杰<sup>2</sup>, 陆企亭<sup>3</sup>, 侯一斌<sup>3</sup>

(1. 复旦大学 材料科学系, 上海 200433; 2. 南京理工大学 软化学与功能材料教育部重点实验室, 南京 210094; 3. 上海康达化工新材料股份有限公司, 上海 201201)

**摘 要:** 以硝酸铜、钼酸钠及氢氧化钠为原料, 采用简单的水相沉淀法, 在 60℃ 下合成出钼铜矿( $\text{Cu}_3(\text{MoO}_4)_2(\text{OH})_2$ ). 通过 X 射线衍射、扫描电镜、透射电镜、热重与差热分析、红外光谱及荧光光谱等测试手段对材料的微观结构、形貌、热稳定性及谱学特性进行表征分析. 结果显示, 制备的产物为结晶性良好的、至少一维是纳米的片状结构材料, 属于单斜型(晶胞参数  $a = 0.53863 \text{ nm}$ ,  $b = 1.40006 \text{ nm}$ ,  $c = 0.56003 \text{ nm}$ ), 其元素摩尔含量比约为 3: 2: 10, 与推测的分子式完全吻合. 热重与差热分析数据表明  $\text{Cu}_3(\text{MoO}_4)_2(\text{OH})_2$  纳米晶具有很好的热稳定性且起始分解温度为 320 ℃. 通过软件测得的  $d_{(021)}$  面与  $d_{(02\bar{1})}$  面的晶间面距分别为 0.435 nm 与 0.358 nm, 与理论值基本相符. 经测量,  $\text{Cu}_3(\text{MoO}_4)_2(\text{OH})_2$  纳米晶具有强的荧光性质, 在激发波长 369 nm 的作用下在 530 nm 表现为强发射峰. 此外, 还探讨了  $\text{Cu}_3(\text{MoO}_4)_2(\text{OH})_2$  纳米晶的形成机理.

**关 键 词:** 钼铜矿( $\text{Cu}_3(\text{MoO}_4)_2(\text{OH})_2$ ); 水相沉淀法; 纳米晶; 表征; 热稳定性; 荧光特性

中图分类号: O782

文献标识码: A